HHS Public Access

Author manuscript

J Leukoc Biol. Author manuscript; available in PMC 2022 May 01.

Published in final edited form as:

J Leukoc Biol. 2021 May ; 109(5): 901–914. doi:10.1002/JLB.2A0520-321RR.

PRDM1 decreases sensitivity of human natural killer cells to IL2-induced cell expansion by directly repressing CD25 (IL2RA)

Burcu Akman[1,2,*], **Xiaozhou Hu**[1,*], **Xuxiang Liu**[3], **Tevfik Hatipoğlu**[1,2], **Hua You**[4,#], **Wing C. Chan**[3,#], **Can Küçük**[1,2,5,#]

[1]İzmir International Biomedicine and Genome Institute (iBG-izmir), Dokuz Eylül University (DEU), İzmir, Turkey

[2]İzmir Biomedicine and Genome Center (IBG), İzmir, Turkey

[3]Department of Pathology, City of Hope, Duarte, CA

[4]Affiliated Cancer Hospital & Institute of Guangzhou Medical University, Guangzhou, China

[5]Department of Medical Biology, Faculty of Medicine, Dokuz Eylül University, İzmir, Turkey

Abstract

IL2 receptor signaling is crucial for human NK cell activation and gain of effector functions. The molecular mechanisms involved in termination of IL2 activation are largely unknown in human NK cells. PR/SET domain 1 (PRDM1) was previously reported to decrease cell growth and increase apoptosis in an IL2-dependent manner in malignant NK cell lines, suggesting the possibility of downregulation of IL2 signaling pathway gene(s) through direct transcriptional repression. Using ChIP-Seq, we identified a PRDM1 binding site on the first intron of *CD25* (*IL2RA*), which codes for the IL2 receptor subunit regulating sensitivity to IL2 signaling, in primary NK cells activated with engineered K562 cells or IL2. Ectopic expression of PRDM1 downregulated CD25 expression at transcript and protein levels in two PRDM1 non-expressing NK cell line. shRNA-mediated knock-down of CD25 in two malignant NK cell lines led to progressive depletion of NK cells in low IL2 concentrations. By contrast, ectopic CD25 expression in primary human NK cells led to progressive increase in cell number in CD25-transduced cells in low IL2 concentrations. Altogether these results reveal a pivotal role of PRDM1 in inhibition of IL2-induced NK cell expansion through direct repression of CD25 in activated human NK cells. These observations provide additional support for the role of PRDM1 in attenuation of NK cell

[#]Correspondence to: Can Küçük, Ph.D., İzmir Biomedicine and Genome Center (IBG), İzmir International Biomedicine and Genome Institute (iBG-izmir), Department of Medical Biology, Faculty of Medicine, Dokuz Eylül University Health Campus, Balcova, 35340 İzmir/TURKEY, Phone: +90 (232) 4126504, can.kucuk@deu.edu.tr; Hua You, Affiliated Cancer Hospital & Institute of Guangzhou Medical University, Guangzhou, China, youhua307@163.com; Wing C. Chan, Department of Pathology, City of Hope, Duarte, CA, jochan@coh.org.

[*]These authors contributed equally.

Author Contributions: B.A., X.H., X.L., and T.H.: performed experiments, analyzed data and wrote the manuscript; Y.H.: wrote the manuscript, and financially supported the study; W.C.C.: assisted in supervision of the experiments, edited the manuscript and financially supported the project; C.K.: conceived, designed, supervised the project, analyzed the data, wrote the manuscript, and financially supported the study.

Conflicts of Interest: The authors declare no conflict of interest.

Supplementary Materials: Four supplementary figures are associated with this manuscript.

activation and growth, with implications on neoplastic transformation or NK cell function when it is deregulated.

Keywords

PRDM1; IL2Rα; CD25; IL2 signaling; natural killer cell expansion

1. Introduction

Interleukin-2 receptor (IL2R) is composed of three distinct non-covalently linked chains, that is, IL2RA (CD25), IL2RB (CD122), and IL2RG (CD132) [1]. Among these proteins, IL2RA is the receptor subunit that increases the affinity of the receptor to IL2 cytokine [2]. IL2 acts in an autocrine manner during development [3] and expansion of T cells [4]. It initiates signaling by recruiting non-receptor tyrosine kinases such as JAK1 and JAK3 to the intracytoplasmic domains of IL2RB and IL2RG, respectively [5]. Importantly, IL2 signaling is involved in differentiation and homeostasis of regulatory T cells (Tregs), and it induces cell growth and proliferation of effector T cells [6]. Preactivation with IL-12, IL-15, and IL-18 was shown to upregulate IL2RA (CD25) expression leading to formation of high affinity IL2R in human cytokine-induced memory-like (CIML) NK cells [7]. This observation suggests the possibility that CD25 upregulation plays a key regulatory role in human NK cell activation by increasing sensitivity of human NK cells to exogeneous IL2.

Natural killer (NK) cells are involved in the eradication of neoplastic, virus-infected or stressed cells [8]. They eliminate their target cells using a well-regulated cascade of events involving direct cell-to-cell contact and release of cytotoxic molecules such as granzyme B and perforin, which destroy their target cells through pore formation in the target cell membrane and apoptosis activation [9]. NK cell activation includes rapid growth and expansion as well as changes in cytokine secretion and cytotoxic capabilities [8]. NK cells can shape the innate and adaptive immune system through secretion of cytokines such as *IFNγ*, *TNFα* to facilitate the eradication of virus-infected or transformed cells [8]. NK cell effector activities can be primed with cytokines including type I interferons (IFNs), IL12 [8], IL2 [10], IL15 [11], IL18 [12] or IL21 [13], which are secreted or trans-presented by the other cellular components of the immune system such as dendritic cells [14]. Of significance, IL2-mediated activation of primary human NK cells showed pleiotropic effects on promoting NK cell activation, which was determined by comparative analyses of gene expression profiles of resting and *ex vivo* IL2 activated NK cells [15]. In particular, IL2 activation induced several genes associated with enhanced cell proliferation, survival and cytokine/chemokine secretion [15]. Interestingly, two recent reports showed an important role of CD25 (IL2RA) in the defense against MCMV infection underscoring the role of IL2 signaling pathway in NK cell activation and growth [16, 17]. Most malignant NK cell lines depend on exogenous IL2 in cell culture medium (Table 1), further emphasizing the importance of IL2 signaling in NK cell survival and proliferation [18, 19].

PRDM1 (BLIMP1) is a transcriptional repressor involved in the differentiation of B cells to plasma cells through transcriptional repression of several genes associated with the B cell

identity, function, and cellular proliferation [20]. PRDM1 is expressed in activated $CD4^+$ and $CD8^+$ T cells, in which it regulates the homeostasis of activated T cells [21, 22]. Importantly, it represses several genes critical in T cell growth such as *IL2* and *FOS* [23], and also genes involved in $CD4^+$ Th1 cell differentiation such as *IFNG*, *TBX21 (TBET)* and *BLC6* [24]. Similar to B cells, it was shown to regulate the terminal differentiation of effector $CD8^+$ T cells [25]. Importantly, sustained expression of CD25 was identified to be responsible for proliferation and survival of Blimp-1-deficient $CD8^+$ T cells in the same study. A core motif of GAAAG and its 5' and 3' nucleotide extended versions have been identified as PRDM1 consensus binding site in a previous report [26].

PRDM1 is located on chromosome 6q21 locus that is frequently deleted in a variety of malignancies including lymphomas and leukemias [27, 28]. Loss-of-function of *PRDM1* due to deletion, mutation, or promoter methylation is frequently observed in B and NK cell malignancies [18, 29, 30]. *In vitro* or *in vivo* functional studies supported the role of PRDM1 as a tumor suppressor gene in activated B-cell (ABC) type of diffuse large B-cell lymphoma (DLBCL) [31, 32], and in natural killer/T cell lymphoma [33, 34]. PRDM1 was reported to be expressed in activated human NK cells [33, 35]. In human NK cells, PRDM1 was shown to directly repress the effector cytokines (i.e. *IFNG*, *TNFA*, *TNFB*) and *CIITA* by binding to conserved motifs [35]. Interestingly, a recent study showed MIR155HG and TERC lncRNAs as indirect transcriptional targets downregulated by PRDM1 in PRDM1-transduced NK cell lines [36].

In the current study, we investigated whether PRDM1 inhibits IL2 signaling through direct transcriptional repression of CD25 (IL2RA) in activated primary human NK cells and NK cell lines using a variety of complementary approaches, and observed the following: **1)** PRDM1 directly bound to the first intron of *IL2RA* in primary human NK cells activated with IL2 or genetically engineered K562 cells; **2)** Ectopic expression of PRDM1α markedly decreased CD25 mRNA and protein expression in two PRDM1 non-expressing NK cell lines with ectopic PRDM1 expression; **3)** Stable knockdown of CD25 inhibited NK cell line growth in low IL2 concentrations; **4)** Ectopic CD25 expression promoted NK cell growth in primary human NK cells when cultured in low IL2 concentrations.

2. Results

2.1. CD25 transcript levels show association with proliferation of primary human NK cells

To address the relationship between CD25 mRNA expression and NK cell expansion capacity, we cocultured peripheral blood lymphocytes with engineered K562 cells (i.e. K562-Cl9-mb21) (Fig. 1A). Consistent with a previous report [33], we observed rapid expansion of NK cells that stopped by day 15 of coculture, which was 3 days after engineered K562 cells were eliminated (Fig. 1B). Interestingly, CD25 transcript levels in these primary NK cells progressively decreased between 13 and 18 days of coculture (Fig. 1C), which suggests that high CD25 levels were associated with expansion capacity of human NK cells. Western blot analyses showed PRDM1 expression in these coculture-activated NK cells at days 12, 15, and 18 (Fig. 1D) as well as at days 10 and 13 (Fig. 1E).

2.2. PRDM1 binds to the first intron of CD25 on activated primary human NK cells

PRDM1/BLIMP1 was reported to inhibit IL2 signaling pathway in vivo by directly repressing IL2 and FOS in late stages of T cell activation [23]. Similarly, ectopically expressed PRDM1 was reported to decrease proliferation and survival of human NK cell lines in low IL2 concentrations, suggesting that it may be targeting gene(s) involved in IL2 signaling pathway [33]. Unlike T cells, human NK cells do not produce IL2 by themselves [37]; suggesting that other genes in IL2 signaling pathway may be targeted by PRDM1. To address this question, we analyzed the ChIP-Seq data to identify PRDM1 binding sites on activated primary human NK cell samples obtained through feeder stimulation (i.e. NKCOD13, NKCOD14) or through stimulation with IL2 (i.e. PBNKD6). Intriguingly, ChIP-Seq peak callers revealed a statistically significant PRDM1 binding site in the first intron of *CD25* (*IL2RA*) in all three NK samples on the following genomic location: Chr10: 6092687–6093005 (human reference hg19) (Fig. 2A). This binding site included PRDM1 consensus sequences (GAAAGT) (Fig. 2B) as identified in previous studies [26]. To cross-validate this ChIP-Seq result, we performed ChIP-qPCR in NKCOD14 cells that showed enrichment of PRDM1 occupancy on Chr10: 6092687–6093005 compared to a negative control site (Fig. 2C).

2.3. CD25 expression is upregulated in activated NK cells and malignant NK cell lines

Next, we evaluated CD25 mRNA expression in primary NK cells activated by IL2 for 2h, 8h, or 24h, and observed upregulation of its expression in NK cells stimulated for 24h (Fig. 3A). To address whether CD25 protein expression levels increase in IL2 activated primary NK cells, we determined surface CD25 expression on primary NK cells with flow cytometry, which showed moderate upregulation of CD25 protein levels in IL2 activated NK cells compared to those in resting NK cells (Fig. 3B). We then evaluated CD25 expression in malignant NK cell lines, most of which were previously shown to have silenced or inactive PRDM1 due to genetic and epigenetic aberrations [18, 33]. CD25 showed higher levels of transcript expression in all malignant NK cell lines (n=9) evaluated compared to the levels in resting NK cells (Fig. 3C). Using flow cytometry, we evaluated CD25 protein expression levels, and observed CD25 overexpression in all malignant NK cell lines evaluated consistent with the transcript levels (Fig. 3D,E).

2.4. Ectopic PRDM1 downregulates CD25 mRNA and protein expression in two PRDM1-null NK cell lines

To address whether PRDM1 transcriptionally downregulates CD25 in PRDM1-transduced PRDM1-null KHYG1 or NK92 cell lines [18], we used a retroviral construct in which PRDM1α and GFP coding sequences are separated with IRES such that GFP expressing cells represent transduced population with ectopic PRDM1 expression (Fig. 4A). We transduced each of these two NK cell lines with empty vector or PRDM1α, and then compared CD25 expression levels using DNA microarray, RNA-Seq, or flow cytometry in FACS-sorted GFP^+ cells two days post-transduction (Fig. 4B). DNA microarray analysis showed that CD25 mRNA expression significantly decreased in KHYG1 or NK92 cell lines transduced with PRDM1α compared to those transduced with empty vector (Fig. 4C). RNA-Seq analyses confirmed transcriptional downregulation of CD25 in NK92 cells transduced

with PRDM1α compared to NK92 cells transduced with the empty vector (Fig. 4D). Next, we performed qRT-PCR to cross-validate downregulation of CD25 in PRDM1α-transduced NK cell lines, and observed significant downregulation of CD25 in both KHYG1 and NK92 cells with ectopic PRDM1α expression (Fig. 4E). To address whether CD25 protein expression levels decrease in these two PRDM1 transduced NK cell line, we evaluated CD25 protein levels with FACS on GFP-gated populations. As expected, ectopic PRDM1 expression downregulated CD25 expression in both NK cell lines compared with empty vector transduced cells (Fig. 4F). Importantly, PRDM1α did not repress IL2RB or IL2RG, which are the two other subunits of the IL2R complex [1], in KHYG1 and NK92 cell lines (Supplementary Fig. S1A, B). Ectopic expression of PRDM1α was shown at mRNA level with RT-PCR (Supplementary Fig. S2B) and protein level with FACS (Supplementary Fig. S2C) in these two NK cell lines.

2.5. CD25 knock-down leads to growth disadvantage in NK cell lines under low IL2 concentrations

Next, we evaluated whether downregulation of CD25 inhibits growth of human NK cell lines cultured in low IL2 concentrations as CD25 was shown in NK cells to increase the sensitivity of the IL2R complex such that NK cells can proliferate under low IL2 concentrations in mice in the presence of viral infections [17]. To address this question, we transduced KHYG1 cells with each of two different CD25 shRNA using a retroviral expression vector that expresses shRNA in mir30 backbone to stably knock-down CD25 expression (Fig. 5A). We then performed a GFP competition assay by tracking GFP^+ cells at consecutive time points after transduction through FACS quantification (Fig. 5B). In relatively high IL2 concentrations (50 IU), there was marginal reduction in CD25 shRNA-transduced KHYG1 cells (Fig. 5C). However, we observed progressive and significant reduction of CD25 shRNA-transduced KHYG1 cells cultured in lower (25 IU) IL2 concentrations for 11 days reflected by the depletion of the GFP^+ cells from unsorted population (Fig. 5D). Next, we transduced another PRDM1-null NK cell line, NK92 [18] with empty vector or either of the two CD25 shRNA, and observed progressive depletion of GFP^+ population in CD25 shRNA-transduced cells but not in empty vector transduced cells when cultured with 25 IU (Fig. 5E) or 12.5 IU (Fig. 5F) of IL2 for 10 days. We tested the efficacy of the CD25 shRNAs by qRT-PCR, and observed 60%−75% CD25 knock-down efficiency in KHYG1 and NK92 cells (Supplementary Fig. S3A, B).

2.6. CD25-transduced primary human NK cells grow faster in low IL2 concentrations

To address whether CD25 expression promotes NK cell growth in low IL2 concentrations, we ectopically expressed CD25 in primary NK cells obtained by coculturing PBL with K562-Cl9-mb21 cells using a retroviral construct in which IRES separates CD25 and GFP coding sequences (Fig. 6A). We performed GFP competition assay on empty vector or CD25-transduced primary NK cells, and determined the GFP positivity with flow cytometry, which showed progressive increase in the percentage of GFP^+ cells in NK cells with ectopic CD25 expression whereas no significant change was observed for empty vector-transduced NK cells (Fig. 6B, C).

3. Discussion

Natural killer cells undergo proliferation and acquire effector functions upon encounter with virus infected [38] or metastatic cells [39]. Appropriate and timely termination of NK cell activation is as important as rapid growth of NK cells during the early response of the host against infectious agents. The mechanisms governing NK cell activation has been relatively well-studied; however, the mechanisms responsible for limiting or terminating NK cell activation are poorly understood. IL2 signaling plays a pleiotropic role in NK cell activation. IL2 signaling was reported to activate a variety of effector functions of NK cells including cytotoxicity [40, 41] and IFN-γ production [42]. NK cells can be induced to proliferate in response to IL2 *in vivo* [10]. A gene expression profiling-based study showed activation of proliferative and survival pathways in *ex vivo* IL2 activated human NK cells [15]. Importantly, most NK cell lymphoma cell lines depend on exogenous IL2 to survive and proliferate [18], and show high CD25 expression (Fig. 3C–E), underscoring the role of CD25 in active IL2 signaling. The fact that IL2 can induce CD25 mRNA expression in primary human NK cells (Fig. 3A) suggests a positive feedback mechanism since a previous report established CD25 (IL2Rα) as an inducible gene of the trimeric IL2 receptor complex in T cells [43]. However, this positive feedback mechanism may not be very prominent for physiological concentrations of IL2 as there is modest increase in CD25 protein expression levels on plasma membrane of IL2 activated primary NK cells (Fig 3B). This observation is consistent with a previous report that showed low proliferation capacity for human NK cells even if they were cultured under very high (1000 U/ml) IL2 concentrations [44]. Our results suggest a pivotal role for PRDM1 in decreasing sensitivity of human NK cells to IL2 through direct transcriptional downregulation of CD25. This finding is also consistent with a previous report that showed decreased cellular growth and increased apoptosis of malignant human NK cell lines transduced with PRDM1 in low IL2 concentrations [33]. By contrast, feeder activated primary human NK cells proliferated and survived better when PRDM1 was silenced using shRNA or CRISPR/Cas9-based systems [33, 45]. Moreover, our observation of promotion of growth of human NK cells by ectopic CD25 in low IL2 concentrations (Fig. 6C) is in line with a previous report showing induction of NK cell proliferation upon selective upregulation of CD25 in mice in response to MCMV infection even in low IL2 concentrations [7].

PRDM1 (Blimp-1 in mice) is a master transcription factor required for terminal differentiation of germinal center B cells to plasma cells through transcriptional repression of genes involved in germinal center B cell function and proliferation [20]. It was shown to regulate homeostasis and function of T cells [21, 22], and to promote $CD8^+$ T cell differentiation through transcriptional regulation of several genes [46]. However, there are only few direct PRDM1 target genes (i.e. *IFN-γ*, *TNF-α*, and *TNF-β*) previously reported in NK cells [35]. The current study extends the list of PRDM1 target genes by establishing *IL2Ra* as a direct target gene in activated primary NK cells, which is transcriptionally downregulated by PRDM1 in human NK cells. Given that PRDM1 protein occupancy on CD25 gene was observed in NK cells activated with IL2 or feeder cells, PRDM1 may be involved in termination of a variety of different NK cell functions through decreasing concentrations of high affinity IL2 receptors on NK cells.

PRDM1 was reported to be up-regulated *ex vivo* by IL2 in primary human NK cells [35]. Interestingly, induction of PRDM1 was slow and progressive in IL2 activated human PB NK cells [33], suggesting that PRDM1 may act as a negative regulator of IL2 signaling in later stages of activation, thereby potentially contributing NK cell homeostasis and regulating its effector functions. Consistent with this possibility, PRDM1 was shown *in vivo* to directly repress *IL2* and the *IL2* activator *FOS* in T cells such that T cell proliferation rate and survival decrease through activation-induced cell death (AICD) [23]. Similar to T cells, PRDM1 may target IL2 signaling during termination of NK cell activation by specifically targeting and decreasing cell surface expression of the alpha subunit of the IL2 receptor, but not the other two subunits. Of note, the extend of CD25 downregulation by PRDM1 in NK cells may be more remarkable than our observations in NK cell lines owing to difficulty in achieving high levels of ectopic PRDM1 expression, as observed for PRDM1 [33, 34] and other tumor suppressors genes [47].

In conclusion, in this study we showed for the first time that PRDM1 transcriptionally downregulates CD25 in human NK cells through direct binding to the first intron of *CD25* using a variety of complementary assays and approaches. This inhibition decreases sensitivity of human NK cells to IL2 such that limiting IL2 concentrations would be insufficient for sustained proliferation and activation of NK cells. Deregulation of this mechanism may promote uncontrolled proliferation, together with the failure of regulation of MYC [48], it may contribute to NK cell malignancies.

4. Materials and Methods

4.1. Malignant cell lines

Malignant NK cell lines and the multiple myeloma cell lines (i.e. U266B1 and IM-9) cell line were cultured in RPMI 1640 (Gibco-Invitrogen, CA, USA) supplemented with 10% FBS, penicillin G (100 units/ml) streptomycin (100 g/ml), and 2 mM L-glutamine at 37 °C in 5% CO2. IL2-dependent NK cell lines were cultured in the presence of 5–7 ng/ml of exogenous rhIL2 (R&D Bioscience, CA, USA). NK92 cells were cultured in 20% FBS. U266B1 cell line was obtained from American Type Culture Collection (TIB-196™, Manassas, VA). IM-9 cell line is a gift from Dr. Anna Scuto (City of Hope). Characteristics of U266B1, IM-9, and NK cell lines (n=9) used in this study are shown in Table 1. 12.5–50 IU (1–4 ng/ml) of IL2 concentrations in NK cell culture medium were considered as low IL2 concentrations whenever applicable.

4.2. Ex vivo activation of human peripheral blood NK cells with IL2

The peripheral blood samples were obtained as buffy coats belonging to healthy blood donors in Blood Bank of Dokuz Eylül University. The IRB approval was obtained from School of Medicine at Dokuz Eylül University with the following IRB approval number: 2018/13–23. PBMCs were isolated from buffy coats using Ficoll-Paque PLUS (GE Healthcare, cat. no. 17144002) according to manufacturer's instructions. Resting NK cells were isolated from the peripheral blood of healthy human subjects using an NK-cell isolation kit (Miltenyi Biotec, Auburn, CA) by applying negative selection as previously described [49]. The purity of NK cells was determined via FACS as > 95% $CD56^{+}/CD3^{-}$

unless otherwise stated. Resting NK cells were activated in the presence of 100 IU/ml of IL2 either for 2, 8, 24 hours or 12, 24, 36 hours to evaluate CD25 transcript expression and protein expression, respectively. CD25 protein expression analysis in IL2 activated primary human NK cells was performed on $CD56^{+}/CD3^{-}$ gated NK cells as they were < 95% $CD56^{+}/CD3^{-}$. Five day IL2 activated peripheral blood NK cells were used as positive control for western blood, whereas 6 day IL2 activated NK cells were used for the ChIP-Seq experiment. NK cells activated with IL2 for 5 or 6 days were referred as PBNKD5 or PBNKD6. IL2 activated NK cells were cultured in a humidified incubator at 37°C and 5% CO2.

4.3. Activation of human peripheral blood NK cells with genetically modified feeder cells

Primary human NK cells were induced to proliferate using a special *ex vivo* system that involves coculturing peripheral blood lymphocytes (PBLs) with the engineered NK cell target (i.e. K562-Cl9-mbIL21). The K562-Cl9-mbIL21 cells were generated from the K562 cell line through genetic engineering to express additional activation molecules (i.e. 4–1BBL, CD86, and membrane-bound IL21), on the cell surface so that NK cells expand rapidly and for an extended period in the presence of IL2 [50]. The full procedure of human NK cell activation through coculturing PBLs with engineered K562 cells are shown in Fig. 1A. Purity of NK cells was evaluated by staining cocultured cells with CD56-PE (Biolegend, San Diego, CA) and CD3-FITC (Biolegend) antibodies using flow cytometry in the 12^{th} and 14^{th} day of coculture. Pure NK cells with ~95% $CD56^{+}$, $CD3^{-}$ phenotype were used in subsequent experiments. Activated primary human NK cells obtained from 13 and 14 days of coculture were referred as NKCOD13 and NKCOD14.

4.4. Western Blot

Western blot was performed as reported previously [18, 33]. Briefly, whole cell extracts from equal number of NK cells cocultured with the engineered K562 cells for 12, 15 and 18 days were resolved in 10% SDS-PAGE gel and transferred to a PVDF membrane. Peripheral blood NK cells activated with IL2 for 5 days (PBNKD5) and KAI3 cells were used as positive and negative controls, respectively [18, 35]. ECL Plus kit (GE Healthcare Bio-Science, NJ, USA) was used to visualize the expression. Anti-PRDM1 (Novus Biologicals, Littleton, CO, USA) antibody was used to detect PRDM1 expression, and α-tubulin (Sigma Aldrich, St Louis, MO) was used as the loading control. The same western blot experiment was repeated with primary NK cells derived from 10 or 13 days of coculture by using the same procedure with the following modifications: GAPDH was used as the loading control. To evaluate expression of PRDM1 and GAPDH, Blimp-1/PRDI-BF1 (C14A4) Rabbit mAb #9115 (Cell Signaling, Danvers, MA, USA) and GAPDH (14C10) Rabbit mAb #2118 (Cell Signaling) were used, respectively.

4.5. ChIP-Seq

For NKCOD13 and PBNKD6, chromatin immunoprecipitation was carried out using the enzymatic ChIP Kit (Magnetic Beads, Cell Signaling, Leiden, The Netherlands), according to the manufacturer's instructions. Briefly, ChIP was performed using $10^{\wedge 7}$ cells for each reaction. For crosslinking, cells were fixed and neutralized using 1% formaldehyde and 125 mM glycine, respectively. To digest the crosslinked chromatin into fragments of 150–900

bp, micrococcal nuclease was used. Diluted DNA fragments (1:5) were incubated with 2μg IgG (Cell Signaling Technology, USA) or PRDM1 (C14A4, Cell Signaling Technology, USA) antibodies. After overnight incubation, PRDM1 antibody-bound chromatin was captured using protein A coated magnetic beads. Crosslinked DNA was eluted from the beads through incubation at 65°C for 30 min and then incubated with proteinase K at 65°C for 3h to reverse the crosslinking. Spin columns were used for the DNA purification.

Library preparation was performed by obtaining DNA fragments through amplification (New England Biolabs, USA) and barcoding as previously described [51]. Amplified products were purified via Agencourt AMPure XP magnetic beads (Beckman Coulter, USA) as reported previously [52]. After clean-up, concentration of the library was approximately 30 nM in 20 ul. Hyper Prep Kit (KAPA, USA) were used for end-repair, adaptor ligation and amplification of PRDM1-ChIP enriched DNA and input DNA Library quantification was tested by qPCR-based techniques. Cluster generation and sequencing were carried out using the Illumina HiSeq 2500 system with a read length of 50 nucleotides.

ChIP was carried out as described previously using NKCOD14 sample [53]. Briefly, ChIP was performed using 6×10^6 cells and 1 μg of specific antibody per immunoprecipitation. The immunoprecipitated DNA was sonicated to fragments of 100–300 bp for ChIP-Seq library preparation. Dynabeads protein A (DynaI Biotech ASA, OSLO, Norway) were incubated with specific ChIP-grade antibodies and the sonicated DNA was pulled down by incubating PRDM1-Ab-dynabead complex with the sonicated lysate overnight at 4°C. The antibodies used were PRDM1 (Cell Signaling, Danvers, MA) and nonspecific rabbit IgG (Santa Cruz Biotechnology, Santa Cruz, CA). The immunoprecipitated DNA was incubated with proteinase K (Roche, Basel, Switzerland) for overnight at 65°C. The ChIP-Seq library was prepared with ChIP-Seq DNA sample prep-kit (IP-102–1001, Illumina Inc., San Diego, CA) using the immunoprecipitated fragments. The fragments with ligated adapters were evaluated for quality control with the Agilent Bioanalyzer 2100. The immunoprecipited DNA were sequenced using Illumina GAIIX sequencing system at UNMC Genomics Core Facility.

4.6. Computational bioinformatics analyses for identification of PRDM1 binding sites

ChIP-Seq peak identification analysis in NKCOD14 cells was performed as described previously [36]. Briefly, CisGenome [54] and MACS [55] ChIP-Seq peak finder programs were used, and statistically significant peaks were identified using the default parameter settings with the following cut-off for significance: FDR<0.01 for CisGenome and $p<10^{-5}$ for the MACS program. Similarly, MACS program was used to identify statistically significant PRDM1 binding sites in NKCOD13 and PBNKD6 as previously reported [56]. Peaks with $p<0.01$ were considered statistically significant. In this study, PRDM1 occupancy only on *CD25* was investigated; the full list of PRDM1 binding sites in NKCOD13, NKCOD14, and PBNKD3 samples will be reported later. The Integrative Genome Browser (IGV) was used to visualize the binding of PRDM1 at the *CD25* (*IL2RA*) genomic region in these three ChIP-Seq samples [57].

We evaluated the statistical significance of the enrichment of the consensus PRDM1 sequences on the genomic region predicted to be occupied by PRDM1 in activated primary

human NK cells through following pipeline. First, PRDM1 consensus sequence file was downloaded from the JASPAR 2020 database (http://jaspar.genereg.net/). The matrix ID of the evaluated PRDM1 consensus sequence file is MA0508.1. Secondly, The DNA sequences for the predicted peak location (Chr10: 6092687–6093005) as well as ± 5000 bp nearby sequences were obtained from the UCSC Genome Browser. Thirdly, as a negative control sequence with no PRDM1 binding on IL2RA based on ChIP-Seq, ~10.000 bp of DNA sequence (chr10: 6065328–6075646) were obtained from UCSC Genome Browser. Fourthly, the sequences as well as the PRDM1 consensus sequence file were uploaded into CentriMo within MEME Suite (http://meme-suite.org/doc/centrimo.html), which is a bioinformatics tool used for identification of consensus motives for transcription factor binding sites. After that, we executed CentriMo program [58] to evaluate whether there is any significant PRDM1 consensus sequence on the genome location predicted to be occupied by PRDM1 on *IL2RA*.

4.7. ChIP-qPCR

The same protocol used for chromatin immunoprecipitation preceding the library prepation step in ChIP-Seq was used for ChIP-qPCR experiments with the following difference: Immunoprecipitated DNA was sonicated to fragments of 100–500 bp for ChIP-qPCR. The functionality of the PRDM1 antibody and the ChIP protocol were tested using U266B1 cells by applying ChIP-qPCR on previously reported known targets of PRDM1 (i.e. *CIITA* pIII, *Tapasin*, and *ERAP1*) [59], which ensured the validity of the ChIP protocol used (Supplementary Fig. S4A). Moreover, immunoprecipitated DNA of NKCOD14 sample was analyzed by quantitative PCR using primers specific for the predicted ChIP-Seq peak location of a previously known PRDM1 binding site on *CIITA* pIV in NKCOD14 sample before ChIP-Seq library preparation (Supplementary Fig. S4B). A genomic location on *SLAMF7* was used as a negative control site during ChIP-qPCR validation for the PRDM1 binding site identified on *CD25* in NKCOD14. ChIP-qPCR primers used in this study are shown in Table 2A.

4.8. Retroviral transduction of NK cell lines

The functional and full-length isoform of PRDM1 (i.e. PRDM1α) [60] was ectopically expressed using the PRDM1α-FL-PMIG construct that was available from previous studies [33]. Retroviral transduction was performed as described earlier [33] with the following modifications: 4 μg of empty vector or PRDM1α-FL was co-transfected with 4 μg of PCL-Ampho, the packaging vector, into the 293T cell line. Transduction efficiency was determined with flow cytometry by determining the percentage of GFP^+ cells 2 days post-transduction.

4.9. DNA microarray

Gene expression profiling was performed on two PRDM1α-transduced, GFP-sorted KHYG1 and NK92 cell lines using HG-U133 Plus 2.0 chips (Affymetrix Inc., Santa Clara, CA) according to the manufacturer's recommendations. The raw data were uploaded into BRB-array tools (version 4.2.1). The Robust Multiarray Average (RMA) method was used to normalize the CEL gene expression values. Genes whose expression did not differ by at least 1.5-fold from the median in at least 20% of the cases were excluded from the analysis.

Normalization and filtering of the microarrays (n=8) representing PRDM1α or empty vector-transduced NK cell lines were performed together with 63 additional arrays. The GEP data of these 8 DNA microarrays used in this study have been deposited into NCBI GEO DataSets with the following registration number: GSE157206. The GEP for the other samples used for normalization were reported in previous studies [18, 61, 62].

4.10. RNA-Seq

RNA-sequencing was performed on empty vector or PRDM1α-transduced NK92 cells. 100 bp paired-end libraries were prepared with the TrueSeq RNA preparation kit (Illumina Inc.), and high throughput sequencing was performed in the UNMC Next Generation Sequencing Core facility. The sequencing reads were aligned to hg19 with Bowtie [63]. Gene expression analysis was performed with the Cufflinks and Cuffdiff [64] programs available inside the Galaxy platform as described previously [36]. Briefly, sequencing reads from empty vector or PRDM1α-transduced NK92 cells were assembled into transcripts using Cufflinks program and BAM alignment files [65]. Cuffmerge program was utilized to annotate and meta assembly the transcripts produced with the Cufflinks. UCSC human reference genome annotation was uploaded to Galaxy and used for the annotation of the transcripts. Cuffdiff program was applied to identify the differentially expressed transcripts with statistical significance. The full profile of the RNA-Seq raw data files are available in NCBI Sequence Read Archive (SRA) database with the following study number: SRP049695.

4.11. qRT-PCR

RNA isolation, reverse transcription and real time PCR were performed as described earlier [33, 49]. Briefly, total RNA was isolated with RNeasy Kit (Qiagen Inc., Gaithersburg, MD), and then reverse transcribed with Stratagene Superscript II reverse transcriptase (Life Technologies Inc., Grand Island, NY) to generate cDNA. Dynamo HS SyBr Green qPCR kit (Thermoscientific Inc., Waltham, MA) was used for the cDNA amplifications. ΔΔCt method was used for relative quantification of the mRNA levels. Melting curves were evaluated to ensure specificity of PCR amplifications. Primers used for qRT-PCR are shown in Table 2B.

4.12. Cell surface CD25 expression analysis with flow cytometry

Empty vector (PMIG) or PRDM1α-FL-PMIG transduced NK92 and KHYG1 cells were stained with CD25-PE (Biolegend, San Diego, CA) antibody according to manufacturer's instruction two days post-transduction. The level of CD25 expression on cell surface of NK cell lines were determined with FACS Aria III flow cytometer using BD FACS Diva 8.0.1 software on GFP gated cells two days post-transduction. CD25 protein expression was evaluated in six malignant NK cell lines and IM-9 cell line using the same flow cytometry procedure except the following difference: CD25 expression was evaluated in all cells of the exponentially growing cell lines. Peripheral blood NK cells were stained with CD56-PE, CD3-APC, and CD25-PE Cy.7 antibodies (Biolegend, USA) following manufacturer's instructions to determine CD25 expression on $CD56^{+}/CD3^{-}$ gated cells.

4.13. Intracellular PRDM1 expression analysis with FACS

Intracellular PRDM1 protein expression in PRDM1α-transduced NK92 and KHYG1 cells was evaluated as follows: Empty vector or PRDM1α-FL-PMIG transduced NK cells were FACS sorted with Aria III flow cytometer two days post-transduction. Before intracellular staining of the sorted GFP^+ cells with PRDM1-APC antibody (R&D Bioscience, CA, USA), cells were fixed and permeabilized using True-Nuclear Transcription Factor Buffer Set (Biolegend, San Diego, CA) according to the manufacturer's instructions. PRDM1 expression levels in transduced KHYG1 and NK92 cell lines were determined via flow cytometer. FlowJo software was used for the analysis of flow cytometry data.

4.14. CD25 short hairpin RNA constructs in NK cell lines

Two 19-mer CD25 siRNAs were designed using the siDESIGN Center (Thermoscientific Inc., Waltham, MA). The siRNA nucleotide sequences were blasted to the human genome to ensure that they do not target other human genes. The siRNAs were converted to 97-mer shRNA-mirs and PCR-amplified with the high fidelity Pfu Ultra II Fusion HS DNA polymerase (Agilent Techonologies, Santa Clara, CA) to directionally clone inside the mir30-adapted retroviral vector, MSCV-LTR-mir30-PIG [66] (LMP) (Addgene plasmid 24071), which was digested with the XhoI and EcoRI restriction enzymes to remove FoxP3 shRNA following the manufacturer's instructions (Thermoscientific Inc., Waltham, MA). The empty MSCV-LMP vector was obtained by removing FoxP3 shRNA which generated XhoI and EcoRI overhangs. The sticky ends were then blunted with the Klenow Fragment (New England Biolabs, Ipswich, MA), and empty LMP was circularized by ligating blunted ends with T4 DNA ligase (New England Biolabs, Ipswich, MA). The sense nucleotide sequences of the siRNAs are as follows: CD25 1^{st} siRNA: 5'-AGGAAGAGTAGAAGAACAA-3'; CD25 2^{nd} siRNA: 5'-CAGAGGAAGAGTAGAAGAA-3'.

4.15. Generation of the retroviral CD25 construct for ectopic expression

CD25 coding sequence (CD25-CDS) was placed into MSCV-IRES-GFP (PMIG) retroviral construct by directional PCR cloning as described earlier [67]. Briefly, PCR cloning primers were designed based on the coding sequence of CD25 (NCBI mRNA accession number: NM_000417.2). NotI and SalI restriction sites were included in the forward and reverse primers, respectively. CD25 coding sequence was amplified from NKYS cell line through high fidelity PCR using PfuUltra II Fusion HS DNA Polymerase (Agilent Technologies, CA, USA). Amplified PCR products were purified with QIAquick PCR Purification Kit (Qiagen, Germany), and also digested simultaneously with NotI and SalI to generate sticky ends. PMIG plasmid was then digested with NotI and SalI. The double-digested and purified CD25 coding sequence (CDS) and PMIG were ligated using T4 DNA ligase (NEB, Germany). Bacterial colonies obtained after heat shock transformation [68] and spread-plating were screened with restriction mapping and Sanger sequencing. Sanger sequencing primers are shown in Table 2C.

4.16. Statistical analysis

The statistical significance of the ChIP-Seq peaks identified on the 1st intron of *IL2RA (CD25) for* PBNKD6, NKCOD13, and NKCOD14 samples are based on the MACS program. Briefly, MACS slides a window across the genome to identify significantly enriched regions compared with the background, followed by merging the candidate regions identified. It models the number of reads from a genomic region as a Poisson distribution with dynamic parameter $\lambda_{\text{local.}}$ MACS assigns every candidate region an enrichment P value on the basis of λ_{local}. The p value for the PRDM1 ChIP-Seq peak identified for PBNKD6 and NKCOD14 are less than 10^{-5}, and the one for NKCOD13 is less than 10^{-2}.

CentriMo, the bioinformatics tool that searches for enriched consensus sequences of transcription factors, applied the binomial test to compute the significance of the number of sequences where the best match occured in a given region by assuming a uniform prior over best match positions. CentriMo reported the location and significance of the best region for the PRDM1 motif. The background model used during motif search normalized for biased distribution of individual letters in evaluated sequences. We chose a 0-order Markov sequence model from the letter frequencies in the primary input sequences. For our analyses, CentriMo also performed comparative enrichment analyses since we provided negative control sequences. As expected, the program identified a PRDM1 consensus site (i.e. DRAAAGTGAAAGTGA) within the center of the predicted ChIP-Seq peak. The p value for the identified peak was 1.1e-3.

The statistical method of the Cuffdiff program, which is a part of the Cufflinks package, was used to evaluate the significance of downregulation of CD25 based on the RNA-Seq data. Cuffdiff's statistical model includes a linear statistical model to estimate an assignment of abundance to each transcript that explains the observed reads with maximum likelihood. This model reports a p value (i.e. q value) corrected for multiple testing. $q<0.05$ was considered statistically significant for the RNA-Seq data.

qRT-PCR, DNA microarray, and FACS data were log-transformed before applying t-test to approximate normal distribution. When the changes in the percentages of GFP+ cells in empty vector versus a relevant gene (i.e. PRDM1 or CD25) or shRNA-transduced cells were evaluated, a paired-t test was applied. $P < 0.05$ was considered significant. Microsoft Office Excel (Microsoft, Redmond, WA) and Prism software package (GraphPad Software, San Diego, CA, USA) were used for t-test.

Supplementary Material

Refer to Web version on PubMed Central for supplementary material.

Acknowledgments:

We'd like to thank Dr. Dean Lee (MD Anderson Cancer Center, Houston) for providing the engineered K562 cells (K562-Clone9-mb21) as well as Müge Özkan and Dr. Gerhard Wingender (İzmir Biomedicine and Genome Center) for sharing us with CD25 FACS antibody.

Funding: This study was supported by Turkish Academy of Sciences, The Outstanding Young Scientists Award (TÜBA GEBİP 2017) to C.K., the National Natural Science Foundation of China grant (81850410547) to Y.H. and the National Institute of Health (NIH) grant (P50CA136411-01/CA/NCI) to W.C.C.

References

1. Smith KA (2006) The structure of IL2 bound to the three chains of the IL2 receptor and how signaling occurs. Medical immunology 5, 3. [PubMed: 16907989]
2. Spolski R, Li P, Leonard WJ (2018) Biology and regulation of IL-2: from molecular mechanisms to human therapy. Nature reviews. Immunology 18, 648–659.
3. Toribio ML, Gutierrez-Ramos JC, Pezzi L, Marcos MA, Martinez C (1989) Interleukin-2-dependent autocrine proliferation in T-cell development. Nature 342, 82–5. [PubMed: 2812004]
4. Feau S, Arens R, Togher S, Schoenberger SP (2011) Autocrine IL-2 is required for secondary population expansion of CD8(+) memory T cells. Nature immunology 12, 908–13. [PubMed: 21804558]
5. Miyazaki T, Kawahara A, Fujii H, Nakagawa Y, Minami Y, Liu Z-J, Oishi I, Silvennoinen O, Witthuhn BA, Ihle JNJS (1994) Functional activation of Jak1 and Jak3 by selective association with IL-2 receptor subunits. 266, 1045–1047.
6. Ross SH and Cantrell DA (2018) Signaling and Function of Interleukin-2 in T Lymphocytes. Annual review of immunology 36, 411–433.
7. Leong JW, Chase JM, Romee R, Schneider SE, Sullivan RP, Cooper MA, Fehniger TA (2014) Preactivation with IL-12, IL-15, and IL-18 induces CD25 and a functional high-affinity IL-2 receptor on human cytokine-induced memory-like natural killer cells. Biology of blood and marrow transplantation : journal of the American Society for Blood and Marrow Transplantation 20, 463–73.
8. Vivier E, Tomasello E, Baratin M, Walzer T, Ugolini S (2008) Functions of natural killer cells. Nature immunology 9, 503–10. [PubMed: 18425107]
9. Smyth MJ, Cretney E, Kelly JM, Westwood JA, Street SE, Yagita H, Takeda K, van Dommelen SL, Degli-Esposti MA, Hayakawa Y (2005) Activation of NK cell cytotoxicity. Mol Immunol 42, 501–10. [PubMed: 15607806]
10. Suzuki R, Handa K, Itoh K, Kumagai K (1983) Natural killer (NK) cells as a responder to interleukin 2 (IL 2). I. Proliferative response and establishment of cloned cells. J Immunol 130, 981–7. [PubMed: 6600260]
11. Lucas M, Schachterle W, Oberle K, Aichele P, Diefenbach A (2007) Dendritic cells prime natural killer cells by trans-presenting interleukin 15. Immunity 26, 503–17. [PubMed: 17398124]
12. Chaix J, Tessmer MS, Hoebe K, Fuseri N, Ryffel B, Dalod M, Alexopoulou L, Beutler B, Brossay L, Vivier E, Walzer T (2008) Cutting edge: Priming of NK cells by IL-18. J Immunol 181, 1627–31. [PubMed: 18641298]
13. Strengell M, Matikainen S, Siren J, Lehtonen A, Foster D, Julkunen I, Sareneva T (2003) IL-21 in synergy with IL-15 or IL-18 enhances IFN-gamma production in human NK and T cells. J Immunol 170, 5464–9. [PubMed: 12759422]
14. Castillo EF, Stonier SW, Frasca L, Schluns KS (2009) Dendritic cells support the in vivo development and maintenance of NK cells via IL-15 trans-presentation. J Immunol 183, 4948–56. [PubMed: 19786554]
15. Dybkaer K, Iqbal J, Zhou G, Geng H, Xiao L, Schmitz A, d'Amore F, Chan WC (2007) Genome wide transcriptional analysis of resting and IL2 activated human natural killer cells: gene expression signatures indicative of novel molecular signaling pathways. BMC Genomics 8, 230. [PubMed: 17623099]
16. Bezman NA, Kim CC, Sun JC, Min-Oo G, Hendricks DW, Kamimura Y, Best JA, Goldrath AW, Lanier LL, Gautier EL, Jakubzick C, Randolph GJ, Best AJ, Knell J, Goldrath A, Miller J, Brown B, Merad M, Jojic V, Koller D, Cohen N, Brennan P, Brenner M, Shay T, Regev A, Fletcher A, Elpek K, Bellemare-Pelletier A, Malhotra D, Turley S, Jianu R, Laidlaw D, Collins JJ, Narayan K, Sylvia K, Kang J, Gazit R, Rossi DJ, Kim F, Rao TN, Wagers A, Shinton SA, Hardy RR, Monach P, Heng T, Kreslavsky T, Painter M, Ericson J, Davis S, Mathis D, Benoist C (2012) Molecular

definition of the identity and activation of natural killer cells. Nature immunology 13, 1000–1009. [PubMed: 22902830]

17. Lee SH, Fragoso MF, Biron CA (2012) Cutting Edge: A novel mechanism bridging innate and adaptive immunity: IL-12 induction of CD25 to form high-affinity IL-2 receptors on NK cells. J Immunol 189, 2712–6. [PubMed: 22888135]
18. Iqbal J, Kucuk C, Deleeuw RJ, Srivastava G, Tam W, Geng H, Klinkebiel D, Christman JK, Patel K, Cao K, Shen L, Dybkaer K, Tsui IF, Ali H, Shimizu N, Au WY, Lam WL, Chan WC (2009) Genomic analyses reveal global functional alterations that promote tumor growth and novel tumor suppressor genes in natural killer-cell malignancies. Leukemia 23, 1139–51. [PubMed: 19194464]
19. Hu X, Chan WC, Kűcűk C (2015) Generation of a genetically engineered aggressive Nk-Cell leukemia cell line with stable IL2 expression. Acta Med. Int 2:78–84
20. Shaffer AL, Lin KI, Kuo TC, Yu X, Hurt EM, Rosenwald A, Giltnane JM, Yang L, Zhao H, Calame K, Staudt LM (2002) Blimp-1 orchestrates plasma cell differentiation by extinguishing the mature B cell gene expression program. Immunity 17, 51–62. [PubMed: 12150891]
21. Martins GA, Cimmino L, Shapiro-Shelef M, Szabolcs M, Herron A, Magnusdottir E, Calame K (2006) Transcriptional repressor Blimp-1 regulates T cell homeostasis and function. Nature immunology 7, 457–65. [PubMed: 16565721]
22. Kallies A, Hawkins ED, Belz GT, Metcalf D, Hommel M, Corcoran LM, Hodgkin PD, Nutt SL (2006) Transcriptional repressor Blimp-1 is essential for T cell homeostasis and self-tolerance. Nature immunology 7, 466–74. [PubMed: 16565720]
23. Martins GA, Cimmino L, Liao J, Magnusdottir E, Calame K (2008) Blimp-1 directly represses Il2 and the Il2 activator Fos, attenuating T cell proliferation and survival. J Exp Med 205, 1959–65. [PubMed: 18725523]
24. Cimmino L, Martins GA, Liao J, Magnusdottir E, Grunig G, Perez RK, Calame KLJTJ o. I. (2008) Blimp-1 attenuates Th1 differentiation by repression of ifng, tbx21, and bcl6 gene expression. 181, 2338–2347.
25. Kallies A, Xin A, Belz GT, Nutt SL (2009) Blimp-1 transcription factor is required for the differentiation of effector CD8(+) T cells and memory responses. Immunity 31, 283–95. [PubMed: 19664942]
26. Doody GM, Care MA, Burgoyne NJ, Bradford JR, Bota M, Bonifer C, Westhead DR, Tooze RM (2010) An extended set of PRDM1/BLIMP1 target genes links binding motif type to dynamic repression. Nucleic Acids Res 38, 5336–50. [PubMed: 20421211]
27. Zhang Y, Matthiesen P, Harder S, Siebert R, Castoldi G, Calasanz MJ, Wong KF, Rosenwald A, Ott G, Atkin NB, Schlegelberger B (2000) A 3-cM commonly deleted region in 6q21 in leukemias and lymphomas delineated by fluorescence in situ hybridization. Genes Chromosomes Cancer 27, 52–8. [PubMed: 10564586]
28. Hyytinen ER, Saadut R, Chen C, Paull L, Koivisto PA, Vessella RL, Frierson HF Jr., Dong JT (2002) Defining the region(s) of deletion at 6q16-q22 in human prostate cancer. Genes Chromosomes Cancer 34, 306–12. [PubMed: 12007191]
29. Tam W, Gomez M, Chadburn A, Lee JW, Chan WC, Knowles DM (2006) Mutational analysis of PRDM1 indicates a tumor-suppressor role in diffuse large B-cell lymphomas. Blood 107, 4090–100. [PubMed: 16424392]
30. Pasqualucci L, Compagno M, Houldsworth J, Monti S, Grunn A, Nandula SV, Aster JC, Murty VV, Shipp MA, Dalla-Favera R (2006) Inactivation of the PRDM1/BLIMP1 gene in diffuse large B cell lymphoma. J Exp Med 203, 311–7. [PubMed: 16492805]
31. Calado DP, Zhang B, Srinivasan L, Sasaki Y, Seagal J, Unitt C, Rodig S, Kutok J, Tarakhovsky A, Schmidt-Supprian M, Rajewsky K (2010) Constitutive canonical NF-kappaB activation cooperates with disruption of BLIMP1 in the pathogenesis of activated B cell-like diffuse large cell lymphoma. Cancer Cell 18, 580–9. [PubMed: 21156282]
32. Mandelbaum J, Bhagat G, Tang H, Mo T, Brahmachary M, Shen Q, Chadburn A, Rajewsky K, Tarakhovsky A, Pasqualucci L, Dalla-Favera R (2010) BLIMP1 is a tumor suppressor gene frequently disrupted in activated B cell-like diffuse large B cell lymphoma. Cancer Cell 18, 568–79. [PubMed: 21156281]

33. Kucuk C, Iqbal J, Hu X, Gaulard P, De Leval L, Srivastava G, Au WY, McKeithan TW, Chan WC (2011) PRDM1 is a tumor suppressor gene in natural killer cell malignancies. Proceedings of the National Academy of Sciences of the United States of America 108, 20119–24. [PubMed: 22143801]
34. Karube K, Nakagawa M, Tsuzuki S, Takeuchi I, Honma K, Nakashima Y, Shimizu N, Ko YH, Morishima Y, Ohshima K, Nakamura S, Seto M (2011) Identification of FOXO3 and PRDM1 as tumor-suppressor gene candidates in NK-cell neoplasms by genomic and functional analyses. Blood 118, 3195–204. [PubMed: 21690554]
35. Smith MA, Maurin M, Cho HI, Becknell B, Freud AG, Yu J, Wei S, Djeu J, Celis E, Caligiuri MA, Wright KL (2010) PRDM1/Blimp-1 controls effector cytokine production in human NK cells. J Immunol 185, 6058–67. [PubMed: 20944005]
36. Baytak E, Gong Q, Akman B, Yuan H, Chan WC, Kucuk C (2017) Whole transcriptome analysis reveals dysregulated oncogenic lncRNAs in natural killer/T-cell lymphoma and establishes MIR155HG as a target of PRDM1. Tumour biology : the journal of the International Society for Oncodevelopmental Biology and Medicine 39, 1010428317701648.
37. Perussia B (1996) The Cytokine Profile of Resting and Activated NK Cells. Methods 9, 370–8. [PubMed: 8812690]
38. Sun JC, Beilke JN, Lanier LL (2009) Adaptive immune features of natural killer cells. Nature 457, 557–61. [PubMed: 19136945]
39. Hanna N and Burton RC (1981) Definitive evidence that natural killer (NK) cells inhibit experimental tumor metastases in vivo. J Immunol 127, 1754–8. [PubMed: 7299115]
40. Kuribayashi K, Gillis S, Kern DE, Henney CS (1981) Murine NK cell cultures: effects of interleukin-2 and interferon on cell growth and cytotoxic reactivity. J Immunol 126, 2321–7. [PubMed: 6164729]
41. Trinchieri G, Matsumoto-Kobayashi M, Clark SC, Seehra J, London L, Perussia B (1984) Response of resting human peripheral blood natural killer cells to interleukin 2. J Exp Med 160, 1147–69. [PubMed: 6434688]
42. Granucci F, Zanoni I, Pavelka N, Van Dommelen SL, Andoniou CE, Belardelli F, Degli Esposti MA, Ricciardi-Castagnoli P (2004) A contribution of mouse dendritic cell-derived IL-2 for NK cell activation. J Exp Med 200, 287–95. [PubMed: 15289500]
43. Lowenthal JW, Bohnlein E, Ballard DW, Greene WC (1988) Regulation of interleukin 2 receptor alpha subunit (Tac or CD25 antigen) gene expression: binding of inducible nuclear proteins to discrete promoter sequences correlates with transcriptional activation. Proceedings of the National Academy of Sciences of the United States of America 85, 4468–72. [PubMed: 3132714]
44. Koehl U, Esser R, Zimmermann S, Tonn T, Kotchetkov R, Bartling T, Sorensen J, Gruttner HP, Bader P, Seifried E, Martin H, Lang P, Passweg JR, Klingebiel T, Schwabe D (2005) Ex vivo expansion of highly purified NK cells for immunotherapy after haploidentical stem cell transplantation in children. Klin Padiatr 217, 345–50. [PubMed: 16307421]
45. Dong G, Li Y, Lee L, Liu X, Shi Y, Liu X, Bouska A, Gong Q, Kong L, Wang J, Lou CH, McKeithan TW, Iqbal J, Chan WC (2020) Genetic manipulation of primary human natural killer cells to investigate the functional and oncogenic roles of PRDM1. Haematologica.
46. Rutishauser RL, Martins GA, Kalachikov S, Chandele A, Parish IA, Meffre E, Jacob J, Calame K, Kaech SM (2009) Transcriptional repressor Blimp-1 promotes CD8(+) T cell terminal differentiation and represses the acquisition of central memory T cell properties. Immunity 31, 296–308. [PubMed: 19664941]
47. Kasof GM, Goyal L, White EJM, biology c. (1999) Btf, a novel death-promoting transcriptional repressor that interacts with Bcl-2-related proteins. 19, 4390–4404.
48. Huang X, S. Q., Fu H1 Zhou X, Guan X, Wang J. (2014) Both c-Myc and Ki-67 expression are predictive markers in patients with extranodal NK/T-cell lymphoma, nasal type: a retrospective study in China. Pathol Res Pract. , 351–6. [PubMed: 24642368]
49. Kucuk C, Hu X, Iqbal J, Gaulard P, Klinkebiel D, Cornish A, Dave BJ, Chan WC (2013) HACE1 is a tumor suppressor gene candidate in natural killer cell neoplasms. The American journal of pathology 182, 49–55. [PubMed: 23142381]

50. Somanchi SS, Senyukov VV, Denman CJ, Lee DA (2011) Expansion, purification, and functional assessment of human peripheral blood NK cells. Journal of visualized experiments : JoVE.
51. Kanai T, Seki S, Jenks JA, Kohli A, Kawli T, Martin DP, Snyder M, Bacchetta R, Nadeau K. C. J. P. o. (2014) Identification of STAT5A and STAT5B target genes in human T cells. 9.
52. Ackermann AM, Wang Z, Schug J, Naji A, Kaestner K. H. J. M. m. (2016) Integration of ATAC-seq and RNA-seq identifies human alpha cell and beta cell signature genes. 5, 233–244.
53. Desai S, Maurin M, Smith MA, Bolick SC, Dessureault S, Tao J, Sotomayor E, Wright K. L. J. M. c. r. (2010) PRDM1 is required for mantle cell lymphoma response to bortezomib. 8, 907–918.
54. Ji H, Jiang H, Ma W, Johnson DS, Myers RM, Wong W. H. J. N. b. (2008) An integrated software system for analyzing ChIP-chip and ChIP-seq data. 26, 1293.
55. Zhang Y, Liu T, Meyer CA, Eeckhoute J, Johnson DS, Bernstein BE, Nusbaum C, Myers RM, Brown M, Li W. J. G. b. (2008) Model-based analysis of ChIP-Seq (MACS). 9, R137.
56. Revilla IDR, Bilic I, Vilagos B, Tagoh H, Ebert A, Tamir IM, Smeenk L, Trupke J, Sommer A, Jaritz M, Busslinger M (2012) The B-cell identity factor Pax5 regulates distinct transcriptional programmes in early and late B lymphopoiesis. The EMBO journal 31, 3130–46. [PubMed: 22669466]
57. Thorvaldsdóttir H, Robinson JT, Mesirov J. P. J. B. i. b. (2013) Integrative Genomics Viewer (IGV): high-performance genomics data visualization and exploration. 14, 178–192.
58. Bailey TL and Machanick P (2012) Inferring direct DNA binding from ChIP-seq. Nucleic Acids Res 40, e128. [PubMed: 22610855]
59. Doody GM, Stephenson S, McManamy C, Tooze R. M. J. T. J. o. I. (2007) PRDM1/BLIMP-1 modulates IFN-γ-dependent control of the MHC class I antigen-processing and peptide-loading pathway. The Journal of Immunology 179, 7614–7623. [PubMed: 18025207]
60. György I, Fejér G, Ghosh N, Seto E, Wright K. L. J. T. j. o. i. (2003) Identification of a functionally impaired positive regulatory domain I binding factor 1 transcription repressor in myeloma cell lines. 170, 3125–3133.
61. Iqbal J, Weisenburger DD, Greiner TC, Vose JM, McKeithan T, Kucuk C, Geng H, Deffenbacher K, Smith L, Dybkaer K, Nakamura S, Seto M, Delabie J, Berger F, Loong F, Au WY, Ko YH, Sng I, Armitage JO, Chan WC (2010) Molecular signatures to improve diagnosis in peripheral T-cell lymphoma and prognostication in angioimmunoblastic T-cell lymphoma. Blood 115, 1026–36. [PubMed: 19965671]
62. Iqbal J, Weisenburger DD, Chowdhury A, Tsai MY, Srivastava G, Greiner TC, Kucuk C, Deffenbacher K, Vose J, Smith L, Au WY, Nakamura S, Seto M, Delabie J, Berger F, Loong F, Ko YH, Sng I, Liu X, Loughran TP, Armitage J, Chan WC (2011) Natural killer cell lymphoma shares strikingly similar molecular features with a group of non-hepatosplenic gammadelta T-cell lymphoma and is highly sensitive to a novel aurora kinase A inhibitor in vitro. Leukemia 25, 348–58. [PubMed: 21052088]
63. Langmead B, Trapnell C, Pop M, Salzberg SL (2009) Ultrafast and memory-efficient alignment of short DNA sequences to the human genome. Genome Biol 10, R25. [PubMed: 19261174]
64. Trapnell C, Roberts A, Goff L, Pertea G, Kim D, Kelley DR, Pimentel H, Salzberg SL, Rinn JL, Pachter L (2012) Differential gene and transcript expression analysis of RNA-seq experiments with TopHat and Cufflinks. Nature protocols 7, 562–78. [PubMed: 22383036]
65. Trapnell C, Williams BA, Pertea G, Mortazavi A, Kwan G, van Baren MJ, Salzberg SL, Wold BJ, Pachter L (2010) Transcript assembly and quantification by RNA-Seq reveals unannotated transcripts and isoform switching during cell differentiation. Nat Biotechnol 28, 511–5. [PubMed: 20436464]
66. Zhou L, Lopes JE, Chong MM, Ivanov II, Min R, Victora GD, Shen Y, Du J, Rubtsov YP, Rudensky AY, Ziegler SF, Littman DR (2008) TGF-beta-induced Foxp3 inhibits T(H)17 cell differentiation by antagonizing RORgammat function. Nature 453, 236–40. [PubMed: 18368049]
67. Hu X, Baytak E, Li J, Akman B, Okay K, Hu G, Scuto A, Zhang W, Kucuk C (2017) The relationship of REL proto-oncogene to pathobiology and chemoresistance in follicular and transformed follicular lymphoma. Leukemia research 54, 30–38. [PubMed: 28095352]
68. Panja S, Saha S, Jana B, Basu T (2006) Role of membrane potential on artificial transformation of E. coli with plasmid DNA. Journal of biotechnology 127, 14–20. [PubMed: 16876281]

69. Tooze RM, Sophie S, Gina MD. Repression of IFN-γ induction of class II transactivator: a role for PRDM1/Blimp-1 in regulation of cytokine signaling. J Immunol. 2006;177.7:4584–4593. [PubMed: 16982896]

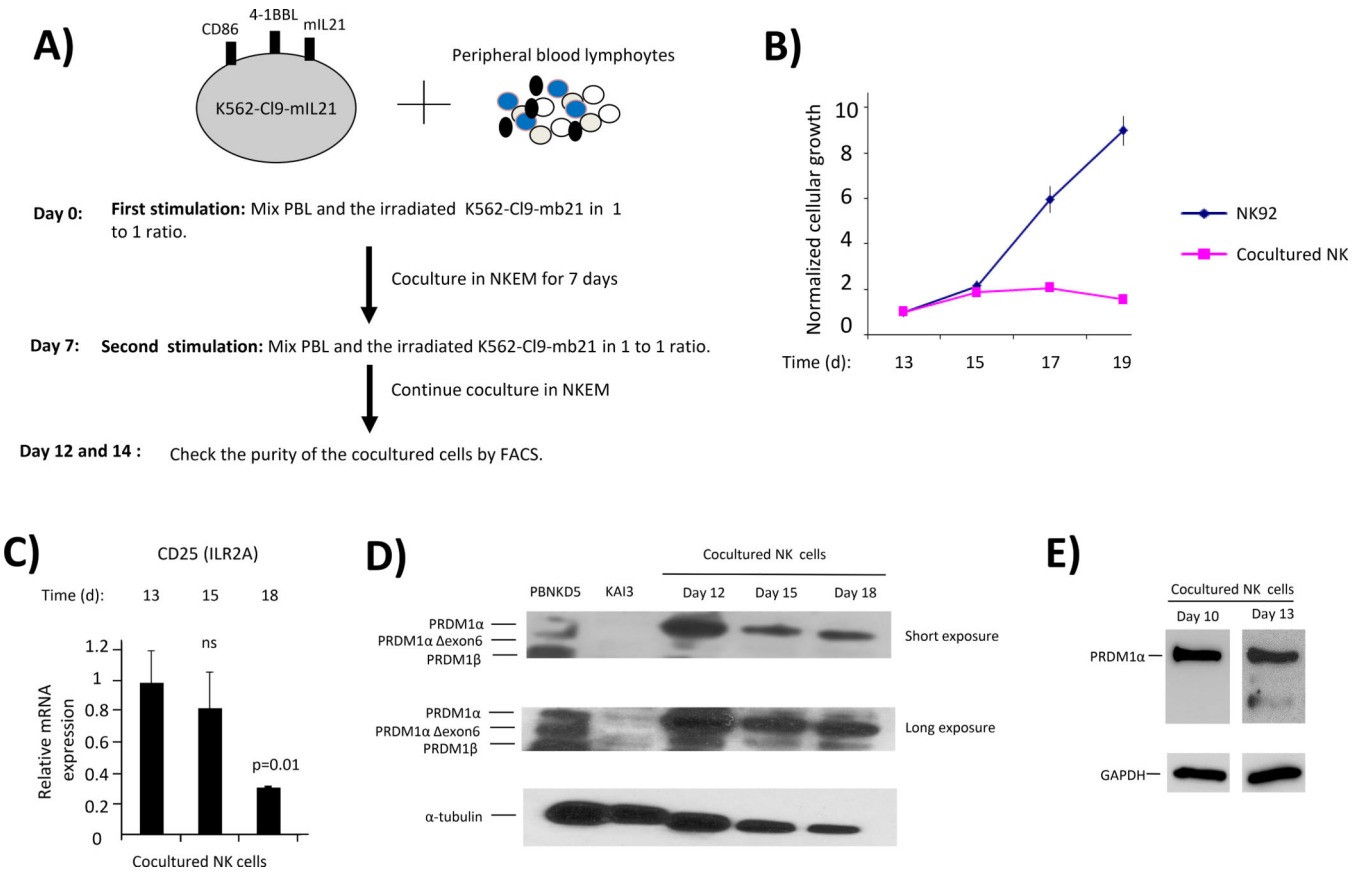

Figure 1. Relationship between CD25 expression levels and the expansion capacity of human primary NK cells.

A) The schematic diagram showing the strategy employed to expand the primary human NK cells by coculturing PBLs with the engineered K562 cells. A modified version of a previously reported (Somanchi et. al. *JOVE* 2011) procedure was employed to expand the human NK-cells. Briefly, equal number of PBLs and 100Gr irradiated K562-Cl9-mb21 cells were seeded together in the presence of the NK-cell expansion medium (NKEM). Seven days after the first induction, equal numbers of cocultured cells were mixed with the 100 Gy irradiated K562-Cl9-mb21 cells and cultured in the presence of the NKEM for 7 more days. The purity of the NK cells was determined with CD56-APC and CD3-PE staining. **B)** The proliferation assay on cocultured NK cells in the later stages of NK cell activation. NK92 cells were used as positive control. Data are means ± SD of two independent experiments. **C)** mRNA expression levels of the CD25 (IL2RA) in NK cells activated with engineered K562 cells during the termination of NK cell activation. RPL13A was used to calibrate the mRNA levels of CD25, and the initial time point of the assay was used to normalize the calibrated expression values. Data are shown as means ± SD. Each data point is representative of replicate measurement of CD25 and RPL13A. The p value was calculated with unpaired t test by comparing the values to those in d13. ns, not significant.Western blot analysis of PRDM1 expression in primary NK cells obtained by coculturing for 12, 15, and 18 days (**D**) or for 10 and 13 days (**E**). Five-day IL2 activated NK cells (PBNKD5) were used as the positive control and PRDM1-null KAI3 cells were used as the negative control.

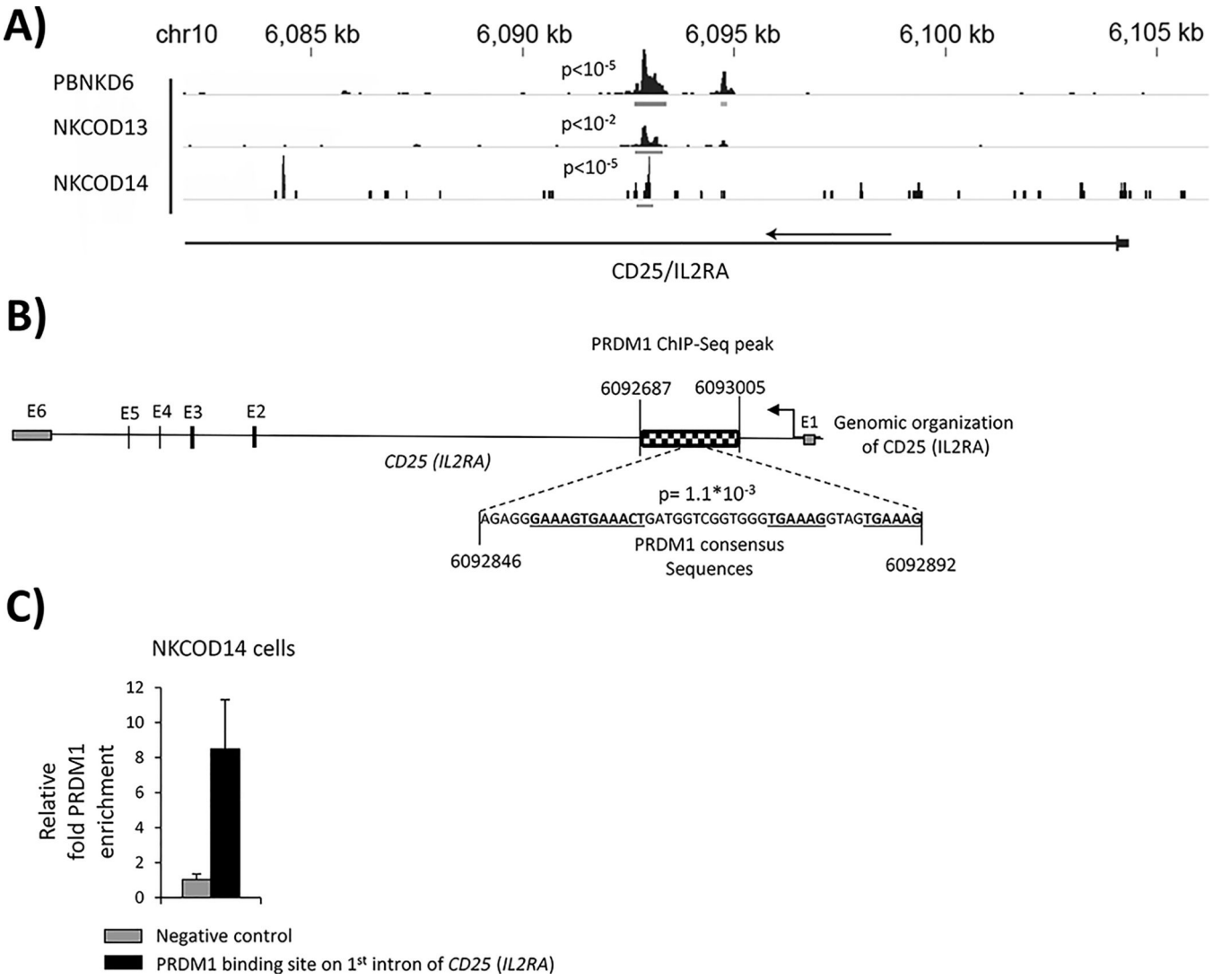

Figure 2. PRDM1 binds to the 1st intron of *CD25* in activated NK cells.

A) The IGV snapshots showing the ChIP-Seq peaks located on the PRDM1 binding site identified downstream of the TSS of CD25 in PBNKD6, NKCOD13, and NKCOD14 samples. Horizontal gray bars indicate the predicted PRDM1 binding sites. The p value was calculated by the MACS program on the basis of the dynamic parameter λ_{local} as described in the Materials and Methods section. **B)** Genomic region of CD25 occupied by PRDM1 in three primary NK samples. The nucleotide sequence for the PRDM1 binding site observed in the CD25 ChIP-Seq peak region was displayed with PRDM1 consensus sites bolded and underlined. The p value was calculated by CentriMo as described in the Materials and Methods section. **C)** ChIP-qPCR cross-validation of PRDM1 occupation on the 1st intron of *CD25* in NKCOD14 sample.

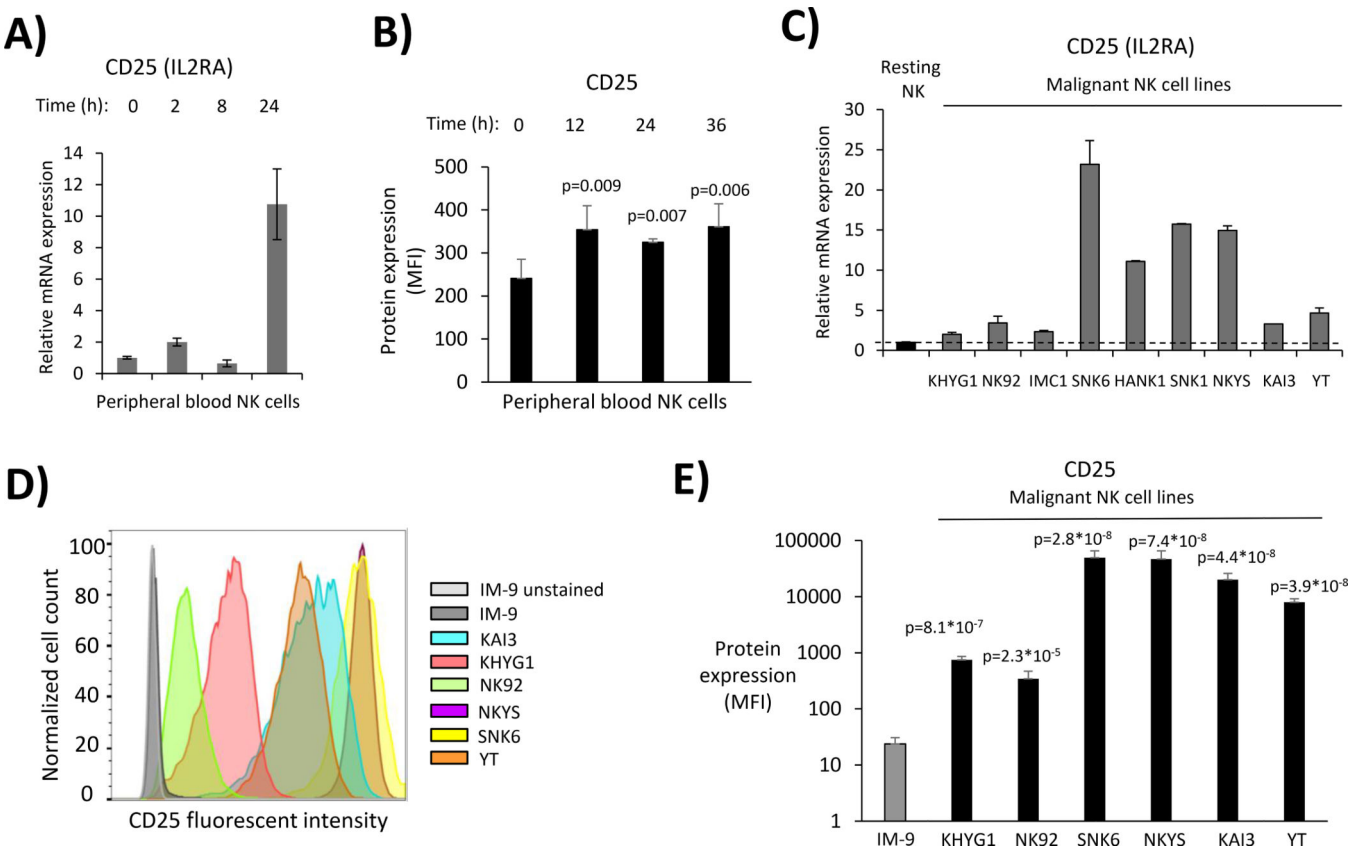

Figure 3. CD25 expression in normal and neoplastic NK cells.

A) CD25 expression was determined with qRT-PCR in primary human NK cells activated by IL2 up to 24h. **B**) The bar graph showing CD25 protein expression levels in resting and IL2 activated primary NK cells, which were determined as mean flourescent intensity (MFI) values with flow cytometry on $CD56^{+}/CD3^{-}$ gated cells. Each data point is average of four measurements derived from two independent experiments with biological replicates. The p values were calculated with unpaired t test by comparing the values to those of 0h time point. **C)** CD25 mRNA expression in 9 malignant NK cell lines were determined with qRT-PCR. RPL13A was used as a reference gene to calibrate CD25 expression. CD25 mRNA expression in resting NK cells were used to normalize the expression level in malignant NK cell lines. The names of NK cell lines are shown below the bar graphs. Data represent means ± SD. **D**) Representative FACS plots showing CD25 protein expression in malignant NK cell lines. **E**) CD25 protein expression levels determined with flow cytometry as MFI values in malignant NK cell lines are shown as a bar graph using logarithmic scale. IM-9, a multiple myeloma cell line with no CD25 expression based on Expression Atlas database (https://www.ebi.ac.uk/gxa/experiments/E-MTAB-2770/Results), was used as the negative control sample. Data represent means ± SD of two independent experiments of which each has biological replicates.

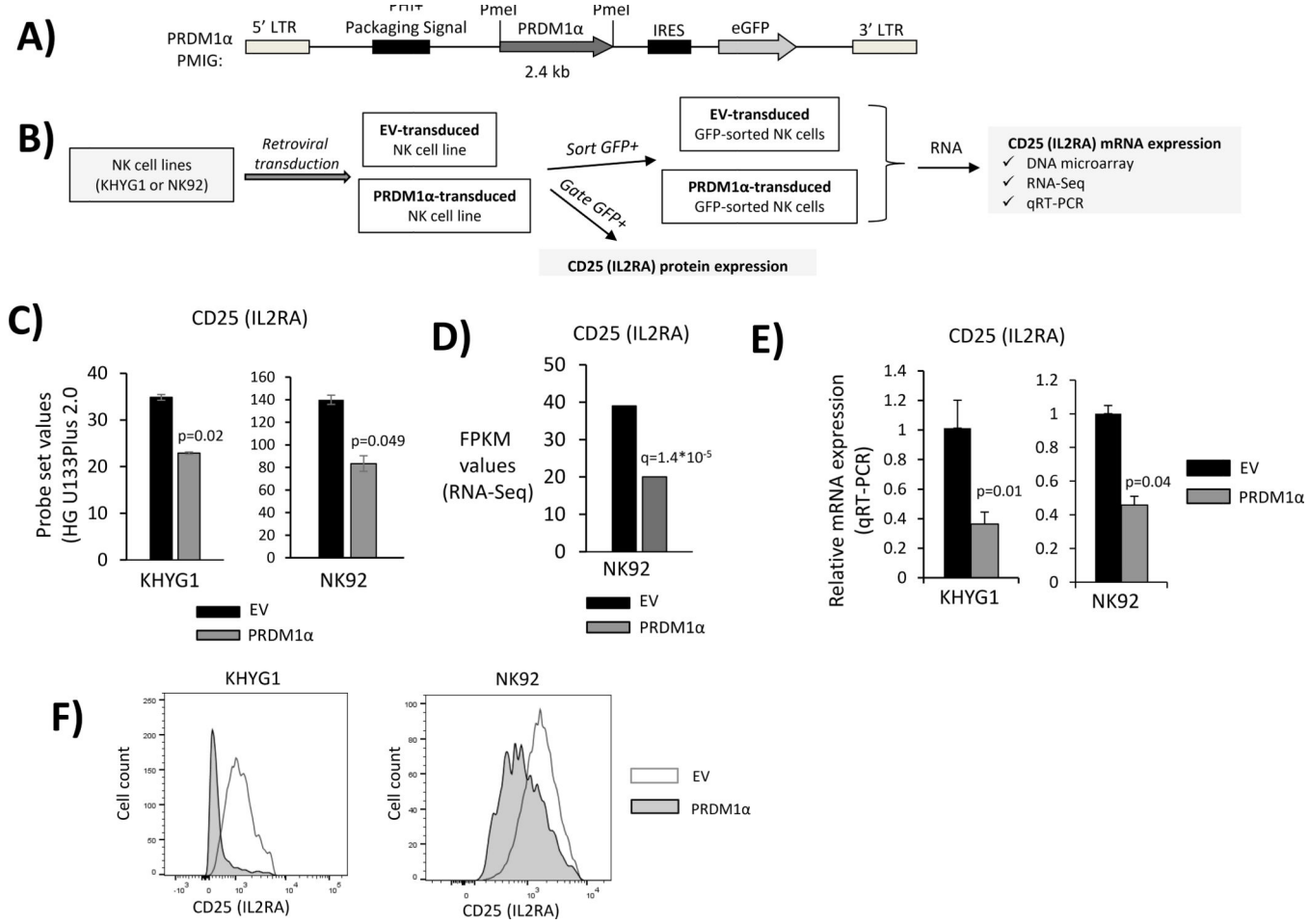

Figure 4. CD25 is transcriptionally downregulated by PRDM1 in PRDM1α-transduced NK cell lines.

A) The retroviral vector used to ectopically express PRDM1α in PRDM1-null NK92 and KHYG1 cell lines. **B)** Schematic representation of the approach used to determine changes in CD25 expression in PRDM1α-transduced NK cell lines. GFP^+ cells were sorted from NK92 or KHYG1 cells 48h post-transduction. Demonstration of transcriptional downregulation of CD25 in PRDM1α-transduced KHYG1 and NK92 cell lines by DNA microarray (**C**), RNA-Seq (**D**) or qRT-PCR (**E**). RNA expression values of PRDM1α-transduced NK cell lines were normalized to the values of the EV-transduced cells. FPKM: Fragments Per Kilobase of transcript per Million mapped reads. For Cuffdiff RNA-Seq expression data, FDR (i.e. q-value), which was obtained after Benjamini-Hochberg correction of the p value is shown. For DNA microarray and qRT-PCR data, paired t test was applied on log2 transformed expression values to obtain p values. **F**) Representative FACS profiles showing the CD25 protein levels of GFP^+ cells in empty vector or PRDM1α transduced NK92 or KHYG1 cells. Each FACS plot is representative of two independent experiments with two biological replicates in each experiment (n=4).

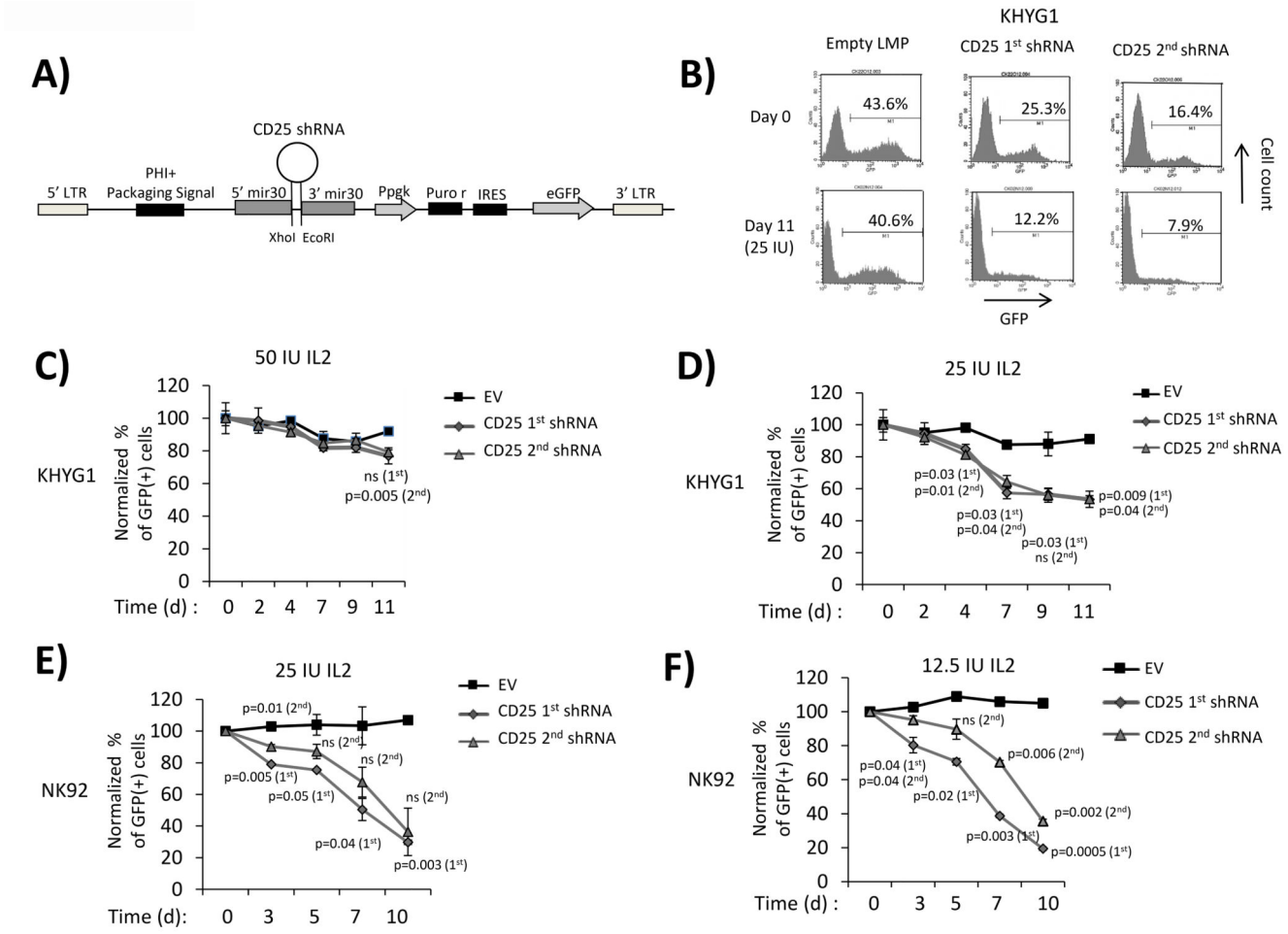

Figure 5. Stable knock-down of CD25 results in decreased cell growth in low IL2 concentrations in malignant NK cell lines.

A) Schematic representation of the retroviral construct used to stably express CD25 shRNA(s) in the context of mir30 backbone. **B)** Representative FACS plots showing the percentage of GFP^+ KHYG1 cells 3 (day 0) or 14 days (day 11) post-transduction with the empty vector or each of two individual CD25 shRNA(s). Transduced KHYG1 cells were cultured in regular IL2 concentrations for 3 days after transduction. Three days after transduction, transduced cells were switched to the NK medium having low doses (50IU or 25IU) of IL2. Day 0 represents the day in which transduced cells were placed in medium with low IL2 concentrations. Three days post-transduction, transduced cells were switched to the NK medium having 50 IU (**C**) or 25 IU (**D**) of IL2. The same experiment was repeated in NK92 cell line starting from Day 0 in which transduced NK92 cell line was switched into culture medium with low IL2 concentrations. The percentage of GFP^+ cells was quantified before and after empty vector or CD25 1st or 2nd shRNA-transduced NK92 cells were placed under culture with 25 IU (**E**) or 12.5 IU (**F**) of IL2. Data represent means ± SD of two independent experiments. The percentage of GFP^+ cells quantified for later time points were normalized to the initial time point of GFP^+ cell quantification. Paired t test was calculated for values in comparison to those of EV-transduced cells for each time point. .

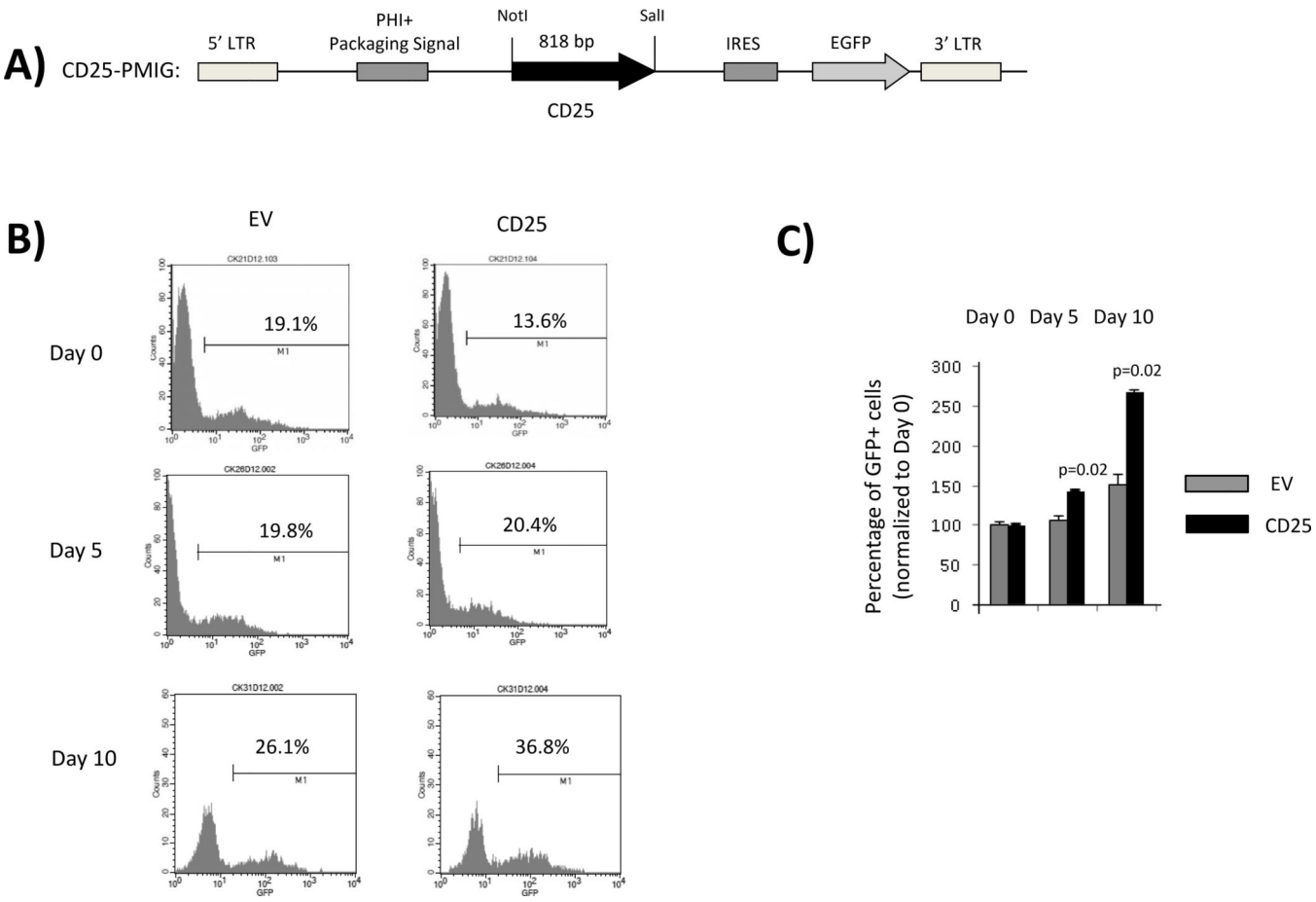

Figure 6. Ectopic expression of CD25 in primary NK cells leads to cellular growth advantage under low IL2 concentrations.

A) Schematic representation of the retroviral construct used for ectopic CD25 expression. **B)** Representative FACS plots of empty vector or CD25-transduced cocultured primary NK cells. The percentage of GFP^+ cells was quantified with FACS four days post-transduction (day 0), and cells were then switched to NK cell culture medium with 12.5 IU IL2 concentrations. **C)** The bar graph showing the relative ratio of GFP^+ cells after normalization to the levels at day 0 for empty vector (EV) or CD25-transduced cocultured NK cells. EV: Empty vector. Data represent means ± SD of two biological replicates. p values were calculated using paired t-test as a comparision to empty vector-transduced sample for each time point.

Table 1.

Characteristics of the human cell lines used in this study

Cell line	Sex	Ethnicity	Original description of disease	CD56	EBV	PRDM1 protein expression status*	Cytokine dependency
KHYG1	F	Japanese	ANKL	+	−	−	IL2
NK92	M	unknown	ANKL	+	+	−	IL2
U266B1	M	unknown	multiple myeloma	N/A	−	+	−
IM-9	F	Caucasian	multiple myeloma	N/A	+	N/A	−
YT	M	Japanese	ALL with thymoma	+	+	−	−
SNK-1	M	Japanese	ENKL	+	+	N/A	IL2
SNK-6	M	Japanese	ENKL	+	+	−	IL2
NKYS	F	Japanese	ENKL	+	+	+	IL2
HANK-1	F	Japanese	ENKL	+	+	N/A	IL2
KAI3	M	Japanese	severe chronic active EBV infection	+	+	−	IL2
IMC1	M	Native American	ANKL	+	−	N/A	IL2

N/A: Not available.

*PRDM1 expression data is based on Iqbal et al. ***Leukemia*** 2009.

Table 2.

Primers used for ChIP-qPCR, qRT-PCR and Sanger sequencing

A) The list of ChIP-qPCR primers used in the study		
	Forward primer	**Reverse primer**
β-globin	5'-TTTTGTTCCCCCAGACACTCTT-3'	5'-GGGTAATCAGTGGTGTCAAATAGGA-3'
SLAMF7	5'-GGCCAGGAAAGTGAAACAGA-3'	5'-TCAGAGCTTAAGTTTGCCATGT-3'
CIITApIII	5'-TCAGTCCACAGTAAGGAAGTGAAATT-3'	5'-GAAACAAGTGAGGGATCATCAAAAA-3'
Tapasin	5'-CCAGGCACCTTCACCTAACC-3'	5'-CAGCCATGAAGCCTCCTCTT-3'
ERAP1	5'-GGATCCGCGTTCAGAAAGG-3'	5'-CCAGGAAGGGAATTGGTAAATG-3'
CIITApIV	5'-GGCCACAGTAGGTGCTTGGT-3'	5'-CTCGTCCGCTGGTCATCCT-3'
B) The list of qRT-PCR primers used to evaluate CD25 expression		
	Forward primer	**Reverse primer**
CD25	5'-AGCGAGCGCTACCCACTTCTAAAT-3'	5'-AGGGTGGAGAGAGTTCCATACCAT-3'
RPL13A	5'-ACCGTCTCAAGGTGTTTGACG-3'	5'-GTACTTCCAGCCAACCTCGTG-3'
C) CD25-PMIG Sanger sequencing primers		
	Forward	**Reverse**
CD25-Sanger-1st	5'-CACGCCAGCCCAATACTTA-3'	5'-GGTGTCACTTGTTTCGTTGTG-3'
CD25-Sanger-2nd	5'-GGACTGCTCACGTTCATCAT-3'	5'-GCTTCTCTTCACCTGGAAACT-3'
CD25-Sanger-3rd	5'- GGATACAGGGCTCTACACAGA-3'	5'-GTGATGTGACTTCAGAGCTTCC-3'

TAPASIN and *ERAP1* primers were reported by Doody et. al. *JI* 2007.

β-globin and *CIITApIII* primers were reported by Tooze et. al. *JI* 2006.

SLAMF7 and *CIITApIV* primers are based on Smith et al *JI* 2010.

RPL13A qRT-PCR primers were reported previously by Küçük et al PNAS 2011.